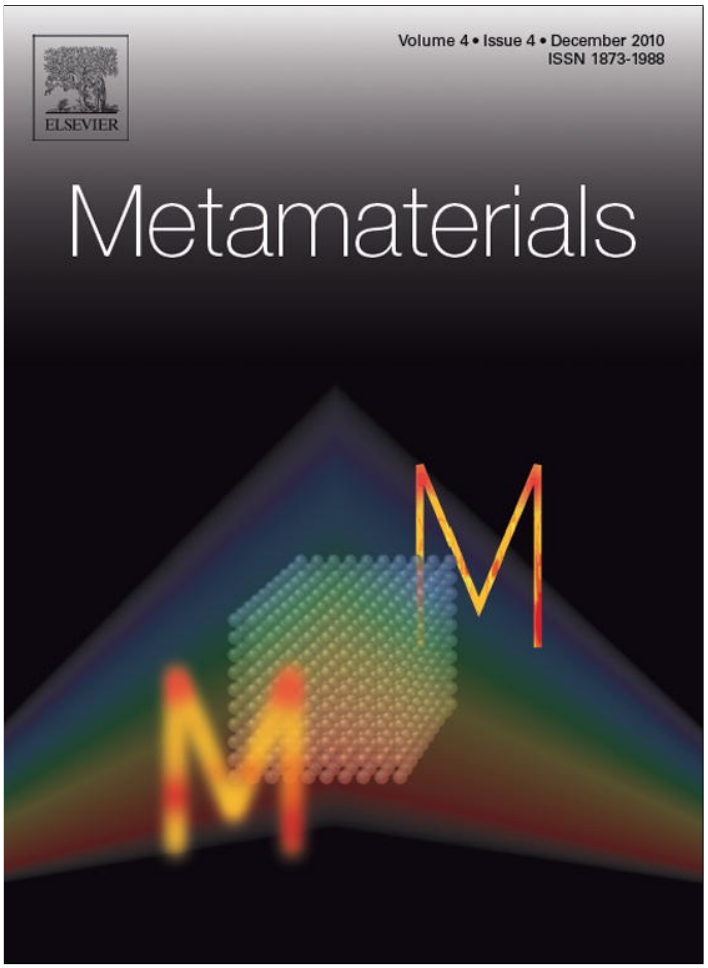

Available online at www.sciencedirect.com
ScienceDirect
Metamaterials 4 (2010) 161–169
Metamaterials
www.elsevier.com/locate/metmat

Bends in magneto-inductive waveguides

R.R.A. Syms *, L. Solymar

Optical and Semiconductor Devices Group, EEE Department, Imperial College London, Exhibition Road, London SW7 2AZ, UK

Received 23 April 2010; received in revised form 25 May 2010; accepted 26 May 2010
Available online 2 June 2010

Abstract

Magneto-inductive (MI) waveguides are periodic structures that operate by magnetic coupling between a set of lumped-element L-C resonators. The effect of waveguide bending on the propagation of MI waves is investigated, and it is shown that discontinuities in axis curvature will typically generate reflections. Changes in the equivalent circuit parameters of two types of MI waveguides (formed from discrete elements and continuous cable, respectively) at abrupt bends are identified, and simple formulae are developed for the reflection and transmission coefficients in each case. It is shown that thin-film MI cable can outperform MI waveguides formed using separate elements, due to the inherent stability of the mutual inductance, and can tolerate extremely tight bends. The theory is confirmed using experiments carried out using thin-film cable operating at ca. 100 MHz frequency.

Keywords: Metamaterial; Magneto-inductive wave; Waveguide bend

1. Introduction

Magneto-inductive (MI) waveguides are low frequency periodic structures that operate by magnetic coupling between lumped-element L-C resonators. To date, two main types have been demonstrated. The first used discrete wire-wound elements mounted on a rod [1,2]. Similar guides used printed circuit board (PCB) elements held in a slotted track [3]. The second used continuously printed arrays of split-ring resonators [4]. However, more practical approaches are required for realistic applications.

Recently, considerable attention has been given to the development of flexible metamaterial for THz applications, and a wide range of resonant elements such as dipoles, Jerusalem crosses, wire pairs and split-ring resonators have been fabricated using single-sided patterning of metal layers on flexible dielectric substrates [5–9]. Larger inductances and capacitances are required at the lower frequencies more typical of MI waveguides, and thin-film magneto-inductive cable has now been demonstrated by using double-sided patterning to construct multilayer capacitors [10]. Such cable has applications where segmentation is required for safety reasons, such as magnetic resonance imaging with an internal detector [11,12]. Several devices based on MI waves have been described, including delay-lines [4], phase shifters [13], passive splitters [14,15], magnetic flux concentrators [16], near-field lenses [17] and ring resonators for detection of MRI signals [18]. However, there has been no work on the effect of bends in magneto-inductive waveguides, although these will be undoubtedly arise in flexible systems.

In other low-frequency RF waveguide systems, discontinuities in axis curvature (for example between

* Corresponding author. Tel.: +44 207 594 6203; fax: +44 207 594 6308.
E-mail address: r.syms@imperial.ac.uk (R.R.A. Syms).

1873-1988/$ – see front matter © 2010 Elsevier B.V. All rights reserved.
doi:10.1016/j.metmat.2010.05.002

straight and curved sections) generally give rise to reflection or (in multi-mode systems) to mode conversion and (at higher frequencies) to radiation. However, for shallow bends at low frequencies the effects are very small, and systems can be constructed using arbitrary cable runs without difficulty. Larger effects are seen with abrupt bends of small radius, which are needed in PCBs. The effects are well understood for microstrip [19–23], coplanar waveguides (CPW) [24,25] and two-wire line [26–29]. Equivalent circuits exist to model bends, mitred corners are used to reduce reflections from microstrip bends [30], and airbridges are used to prevent mode conversion in CPW bends [31]. Comparable analyses and solutions are clearly required for magneto-inductive waveguides.

In this paper, we present an initial investigation of bends in magneto-inductive waveguides. We begin in Section 2 by identifying the effect of abrupt bends on the equivalent circuit parameters of two types of magneto-inductive guide, formed from discrete elements and as continuous cable, respectively, and show that the latter are inherently more stable. In Section 3, we develop a simple model for the reflection from bends of each type. In Section 4 we verify the model using experiments on magneto-inductive cables operating at low (ca. 100 MHz) frequency. Conclusions are presented in Section 5.

2. Magneto-inductive waveguides and bends

In this section, we briefly review the properties of magneto-inductive waveguides, and then consider the format of bends in guides based on discrete elements and continuous cable.

2.1. MI waveguides

Fig. 1a shows a one-dimensional magneto-inductive waveguide, which consists of a set of L-C resonators coupled by mutual inductances M [1,2]. Assuming there is no loss, and that only nearest neighbours are coupled, the equations governing the current I_n in the nth element at angular frequency ω is:

$$\{j\omega L + 1/j\omega C\}I_n + j\omega M(I_{n+1} + I_{n-1}) = 0 \qquad (1)$$

Assuming a travelling wave solution as $I_n = I\exp(-jkna)$, where k is the propagation constant and a is the element separation, Eq. (1) yields the

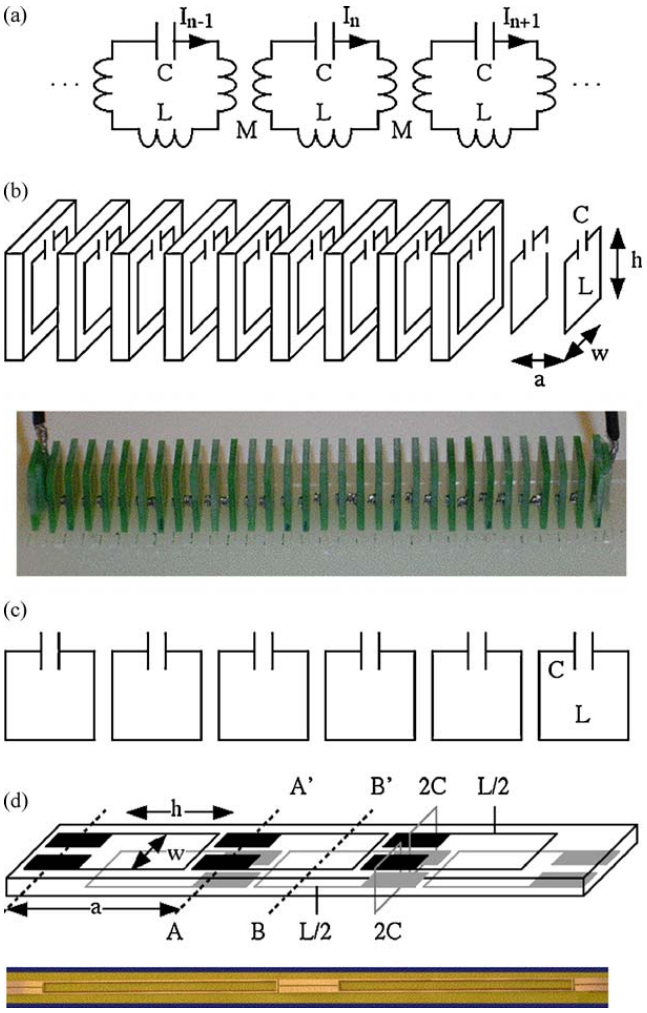

Fig. 1. Magneto-inductive waveguides: (a) equivalent circuit, (b and c) guides based on discrete elements arranged in axial and planar configurations; (d) thin-film cable.

dispersion equation:

$$\left\{1 - \frac{\omega_0^2}{\omega^2}\right\} + \kappa\cos(ka) = 0 \qquad (2)$$

Here $\omega_0 = 1/(LC)^{1/2}$ is the angular resonant frequency, $f_0 = \omega_0/2\pi$ is the corresponding temporal frequency and $\kappa = 2M/L$ is the coupling coefficient.

A magneto-inductive guide can support forward or backward waves, when the mutual inductance M (and hence also the coupling coefficient κ) is positive or negative, respectively. In the former case, propagation takes place in a band ranging from $1/\sqrt{(1+\kappa)} \le \omega/\omega_0 \le 1/\sqrt{(1-\kappa)}$. If loss is included in the model, the propagation constant becomes complex, so that $k = k' - jk''$. For small losses $k''a \approx 1/\{\kappa Q\sin(k'a)\}$, where $Q = \omega L/R$ is the Q-factor of the elements and R is the loop resistance. Consequently, low propagation loss requires strongly coupled elements

with a high Q-factor. A non-reflective termination can be formed by inserting an impedance $Z_0 = j\omega M \exp(-jka)$ into the final element. At mid-band, when $\omega = \omega_0$ and $ka = \pi/2$, Z_0 reduces to the real value $Z_{0M} = \omega_0 M$, allowing a magneto-inductive waveguide to be coupled to a resistive load.

2.2. Waveguides formed from discrete elements and as continuous cable

Fig. 1b and c shows magneto-inductive guides based on discrete elements in the axial and planar configurations (which support forward and backward waves, respectively). In each case, the element is formed from an inductor L and a capacitor C. Strong coupling with a maximum possible value of $\kappa = 2$ (axial) and $\kappa = -1$ (planar) is obtained if the elements are placed close together. Since the element separation must then be small, losses per metre may then still be high. In addition, second nearest neighbour interactions will almost certainly become significant [32].

Fig. 1d shows thin-film cable [10], which supports forward waves. Each element is now realised using a pair of series-connected inductors of value $L/2$ and a pair of series-connected capacitors $2C$. The capacitors are formed as parallel plate components, using a very thin flexible substrate as a dielectric interlayer. The inductors are overlaid on either side of the substrate, so that strong coupling is inherently obtained. Although the maximum possible coupling strength is reduced to $\kappa = 1$, losses per metre can be much lower because of the larger element separation, and second neighbour effects are minimal.

Each type of guide can be modelled using Eqs. (1) and (2), and each may be formed into a bend by a variation in the propagation axis. At the low operating frequencies of typical MI systems there will be little radiation loss. Instead, the main effect of bending will be to generate reflections. We now consider the mechanism for reflection in each case.

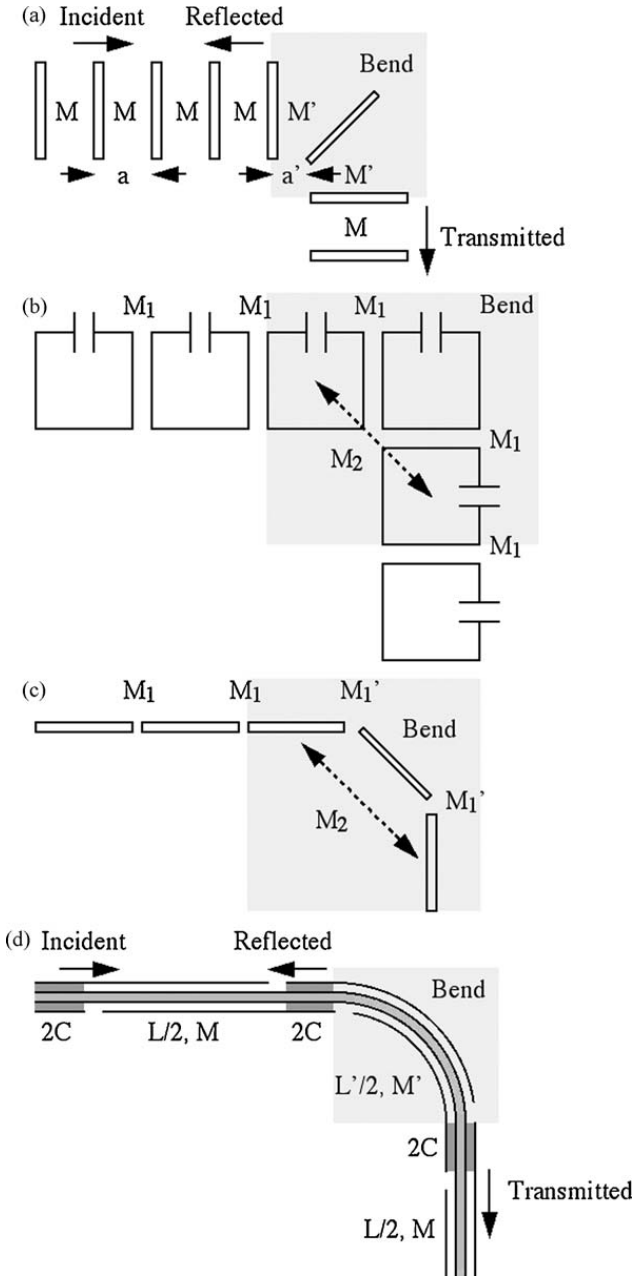

Fig. 2. Magneto-inductive waveguide bends based on discrete resonant elements in (a) the axial configuration, (b and c) the planar configuration and (d) thin-film cable.

2.3. Bends in discrete-element waveguides

Because propagation losses are typically high in MI systems, we focus on arrangements that involve only a small number of elements. An abrupt 90° bend in a discrete system can be realised by changing the orientation of the elements. For discrete-element guides, the results are as shown in Fig. 2. For the axial configuration with circular or square elements, only one distinct bending axis need be considered (Fig. 2a). However, the insertion of an element inclined at 45° to the propagation axis is really required at the bend, to avoid a drastic change in local properties. For the planar configuration, there are two possible bending axes (Fig. 2b and c). For in-plane bending, only a change in element position is needed. For out-of-plane bending, a change in element orientation is again involved, and insertion of additional inclined elements is likely to be beneficial.

In each case, L and C are unaltered, so the resonant frequency f_0 must remain constant. However, the mutual inductance can certainly change. For the axial configuration, the mutual inductance between near neighbours

may change to M' near the inclined element. For the planar configuration with in-plane bending, it is simple to hold the mutual inductance M_1 between nearest neighbours constant. However, significant mutual inductance M_2 may arise between non-nearest neighbours. For out-of-plane bending, there are again likely to be changes in nearest-neighbour effects. These may be cancelled to first order using a mechanical linkage developed for flexible MI ring resonators [18], which can adjust the separation of inclined elements to compensate for changes in angle. However, as has previously been shown, it is not possible to compensate for second neighbour effects.

Because of the complications arising from second neighbour effects, we focus on the axial configuration. To avoid reflections, M' should equal M as far as possible. This requirement imposes constraints on the relative values of the spacing a and a' in the straight and bent sections. We illustrate the constraints by using the freeware numerical simulation tool FASTHENRY [33] to estimate the self- and mutual inductance obtained with elements based on single-turn square inductors. The assumed dimensions were a loop width $w = 20$ mm and height $h = 20$ mm, and a conductor track width and thickness of 0.5 mm and 0.035 mm, respectively. Fig. 3a shows the variation of the coupling coefficient with element spacing, assuming that the elements are firstly parallel and secondly inclined at 45° to each other. In the former case, κ reduces monotonically with a/w from a maximum of 2 at small separation. In the latter, κ falls from a much lower maximum of ≈0.63. However, the functional forms are not identical and M'/M rises slowly from ≈0.32 to 0.5 over the range shown.

The straight-line construction shows how discontinuities in κ may be avoided in a bend. Starting with the minimum practical separation (here, assumed to be 2 mm, so that $a'/w = 0.1$) the value of the coupling coefficient in the bend is read off (here, as around 0.28). The separation giving the same value of κ in the straight section is then found (here, as around $a/w = 0.35$, so that $a = 7$ mm). If these two different values of element separation are used in the straight and bent sections of the waveguide, the bend will then present no discontinuity in mutual inductance. This construction shows that arrangements that avoid discontinuities can be found in principle. However, because the element spacing must then be precisely defined along the entire length of the guide, these will be difficult to achieve in practice. In addition, the reduced mutual inductance of inclined elements implies that the coupling coefficient everywhere must then be relatively small, so that propagation losses will be high.

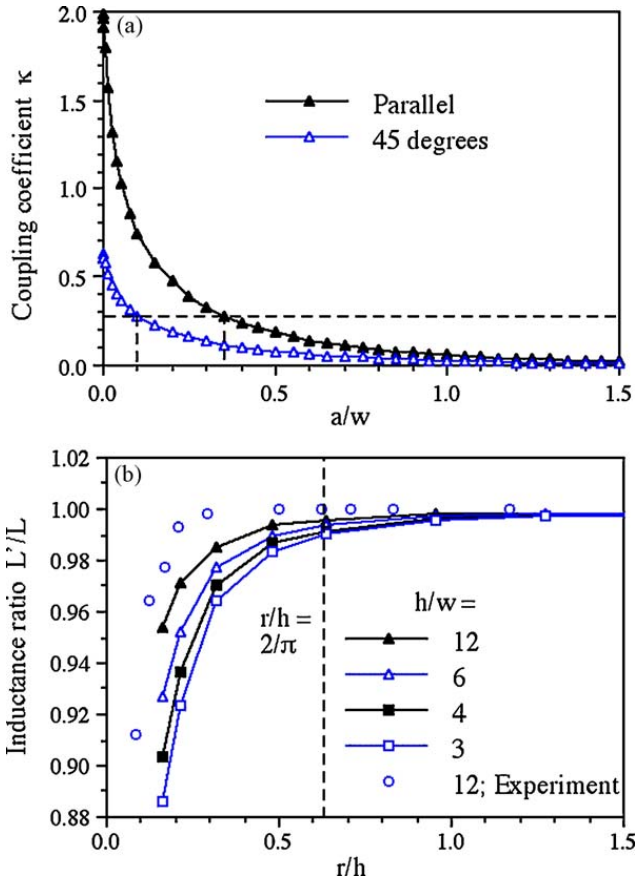

Fig. 3. (a) Variation of the coupling coefficient between parallel and inclined elements with normalised separation for discrete resonant elements in the axial configuration; (b) variation of normalised inductance L'/L with normalised bend radius r/h for cable.

2.4. Bends in continuous cable

Using thin-film cable, a bend can only be realised if the elements are physically distorted. Bending can now only take place about one axis. However, this is not an important restriction since twisting can provide the additional degree of freedom needed for arbitrary pathways. In this case, the position and length of the bend will alter the outcome. If the axis of the bend passes through the capacitors (for example, along the line A–A' in Fig. 1d) and the bend is limited therein, there will be hardly any effect. One way to minimise bending effects might therefore be to stiffen the cable near the inductors, so that deformation is restricted to the capacitors. Alternatively, if the axis passes through the inductors (for example, along B–B') we might expect to see changes in inductance in two adjacent elements. Fig. 2d shows a symmetric 90° bend formed in this way. In this case f_0 can alter, and variations in f_0 will again generate reflections. However, since the inductors of adjacent elements are intimately connected, self- and mutual inductances are likely to alter at almost exactly the same rate.

To see the effects, simulations were again carried out using FASTHENRY, this time assuming rectangular inductors with a length $h = 60$ mm, and a conductor width and thickness of 0.5 mm and 0.035 mm. Long conductors were sub-divided into 12 sections, whose relative orientations could be altered to simulate an inductor bent into a circular arc. Calculations were carried out for different arc radii (i.e. without restricting the bend angle to 90°), using different values of the aspect ratio h/w. Fig. 3b shows the variation of the ratio L'/L with the normalised bend radius r/h. The inductance is approximately constant for large r/h, but starts to fall when $r/h < 0.5$. The effect is delayed and reduced for larger h/w, i.e. for longer, thinner inductors. However, the reduction is in all cases small, and only around 1% when $r = 2h/\pi$ (a 90° bend).

These results are in qualitative agreement with earlier findings for the reduction in inductance caused by bends in two-wire line [27]. The implication is, somewhat surprisingly, that the inductance of a long, thin inductor is very stable against bending. Consequently, the effect of distorting a cable should be limited to small changes in f_0 and even smaller changes in M/L. It is therefore unlikely that the complicated compensation described above for a discrete-element bend will be required.

3. Reflections from bends

In this section, we consider the reflection that must arise at the discontinuity between straight and curved magneto-inductive waveguides, using the models for discrete and continuous systems introduced in the previous section.

3.1. Discrete elements

The effect of a bend on wave propagation may be modelled by assuming a locally modified equivalent circuit. For a guide formed using discrete elements in the axial configuration, the circuit is as shown in Fig. 4a. Here the bend is located in element 0, and the mutual inductance to neighbours on either side is simply modified from M to M'. Away from the bend, Eq. (1) is still valid, but the circuit equations for elements −1, 0 and +1 are now:

$$\begin{aligned} \{j\omega L - 1/j\omega C\}I_{-1} + j\omega\{M'I_0 + MI_{-2}\} &= 0 \\ \{j\omega L - 1/j\omega C\}I_0 + j\omega M'\{I_1 + I_{-1}\} &= 0 \\ \{j\omega L - 1/j\omega C\}I_1 + j\omega\{MI_2 + M'I_0\} &= 0 \end{aligned} \tag{3}$$

Since these equations are similar to ones used in [15] to describe magneto-inductive Fabry–Perot resonators, we would expect similar behaviour. Solutions away from the junction are assumed in the form of incident, reflected and transmitted waves, as:

$$\begin{aligned} I_n &= I\exp(-jkna) + R\exp(+jkna) \quad n \le -1 \\ I_n &= T\exp(-jkna) \quad n \ge +1 \end{aligned} \tag{4}$$

Here R and T are unknown coefficients, as is the current I_0. Eq. (4) satisfy Eq. (1) automatically. Substituting into Eq. (3), using the dispersion equation and eliminating I_0, the reflection and transmission coefficients $\Gamma = R/I$ and $T = T/I$ can be found as:

$$\begin{aligned} \Gamma &= \frac{(1-\mu^2)\{\exp(+jka) + \exp(-jka)\}}{(2\mu^2 - 1)\exp(-jka) - \exp(+jka)} \\ T &= \frac{\mu^2\{\exp(-jka) - \exp(+jka)\}}{(2\mu^2 - 1)\exp(-jka) - \exp(+jka)} \end{aligned} \tag{5}$$

Here $\mu = M'/M$. It is simple to show both analytically and numerically that the solutions conserve power, so that $\Gamma\Gamma^* + TT^* = 1$. The reflection and transmission coefficients depend only on μ and the propagation constant. The reflection clearly vanishes if $\mu = 1$, i.e. if there is no discontinuity. If we now assume that M'/M is close to unity, so that $\mu = 1 + \varepsilon$, where ε is small, a first-order approximation to the reflection coefficient may be found

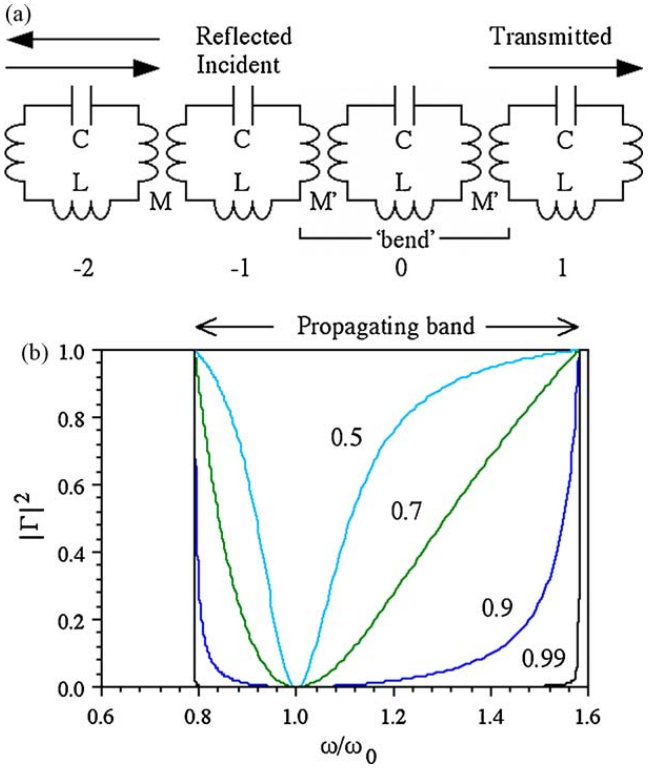

Fig. 4. (a) Equivalent circuit for a bend in an axial magneto-inductive waveguide based on discrete elements; (b) frequency variation of the power reflection coefficient $|\Gamma|^2$ for different values of the inductance ratio $\mu = M'/M$.

as:

$$\Gamma = \frac{-2j\varepsilon\,\cos(ka)}{\sin(ka)} \tag{6}$$

Numerical evaluation shows that this solution is indeed a reasonable approximation, except near the band edges. It implies that the reflection will be proportional to the fractional discontinuity in M, minimum at the band centre ($ka=\pi/2$, or $\omega=\omega_0$) and maximum at the band edges ($ka=0$ or π).

Fig. 4b shows the exact frequency variation of the power reflection coefficient $|\Gamma|^2$, for the example parameters of $\kappa=0.6$ and different values of μ. For this value of coupling strength, propagation takes place in the band $0.79<\omega/\omega_0<1.58$. For $\mu\approx1$, the reflection is low except near the band edges, and zero at $\omega=\omega_0$. As μ departs further from unity, the reflection increases everywhere except at $\omega=\omega_0$, so that the bend does indeed start to act as a Fabry–Perot cavity, transmitting only at one frequency. This behaviour highlights two important features of magneto-inductive waveguides formed from discrete elements, namely etalon effects in poorly designed bends and the need for a general reduction in coupling coefficient (and a consequent increase in propagation loss) to avoid such affects.

3.2. Continuous cable

Fig. 5a shows the corresponding equivalent circuit for a bend in thin-film cable, located in elements −1 and 0. Now we assume that the relevant component values alter from $L/2$ to $L'/2$ and from M to M'. Assuming that the self- and mutual inductance alter at the same rate, we can write $L'/L=M'/M=\mu$. Away from the bend, the circuit equations are again as Eq. (1). However, for elements −1 and 0 they modify to:

$$\begin{aligned}\{j\omega L(1+\mu)/2+1/j\omega C\}I_{-1}+j\omega M\{\mu I_0+I_{-2}\}=0\\ \{j\omega L(1+\mu)/2+1/j\omega C\}I_0+j\omega M\{I_1+\mu I_{-1}\}=0\end{aligned} \tag{7}$$

Assuming solutions in terms of incident, reflected and transmitted waves as before, the reflection and transmission coefficients can be obtained for this case as:

$$\begin{aligned}\Gamma&=\frac{-\{\kappa^2(1-\mu^2)+(1-\mu)^2\}\exp(+jka)-\kappa(1-\mu)\{1+\exp(+j2ka)\}}{2\kappa(1-\mu)+\kappa^2\exp(+jka)+\{(1-\mu)^2-\mu^2\kappa^2\}\exp(-jka)}\\ T&=\frac{\mu\kappa^2\{\exp(+jka)-\exp(-jka)\}}{2\kappa(1-\mu)+\kappa^2\exp(+jka)+\{(1-\mu)^2-\mu^2\kappa^2\}\exp(-jka)}\end{aligned} \tag{8}$$

Eq. (8) are similar to Eq. (5), but now contain the coupling coefficient κ. Again, it can be shown that these solutions conserve power. Putting $\mu=1+\varepsilon$ once again, an approximation for the reflection coefficient valid for small discontinuities may be found as:

$$\Gamma = \frac{-j(\varepsilon/\kappa)\exp(jka)\{\cos(ka)+\kappa\}}{\sin(ka)} \tag{9}$$

Eq. (9) implies that the reflection coefficient will again be proportional to the fractional discontinuity, and will increase at the band edges. However, Γ will now be zero at the frequency for which $\cos(ka)+\kappa=0$, namely $\omega=\omega_0/\sqrt{(1-\kappa^2)}$, rather than at $\omega=\omega_0$. Fig. 5b shows the exact frequency variation of the power reflection coefficient $|\Gamma|^2$, for $\kappa=0.6$ and different values of μ. These plots are qualitatively similar to, but differ in detail from, those in Fig. 4b. Once again, for $\mu\approx1$, the reflection is again low except near the band edges, and zero at $\omega=\omega_0$. As μ departs further from unity, the reflection increases everywhere except at an optimum frequency, which gradually shifts to higher values.

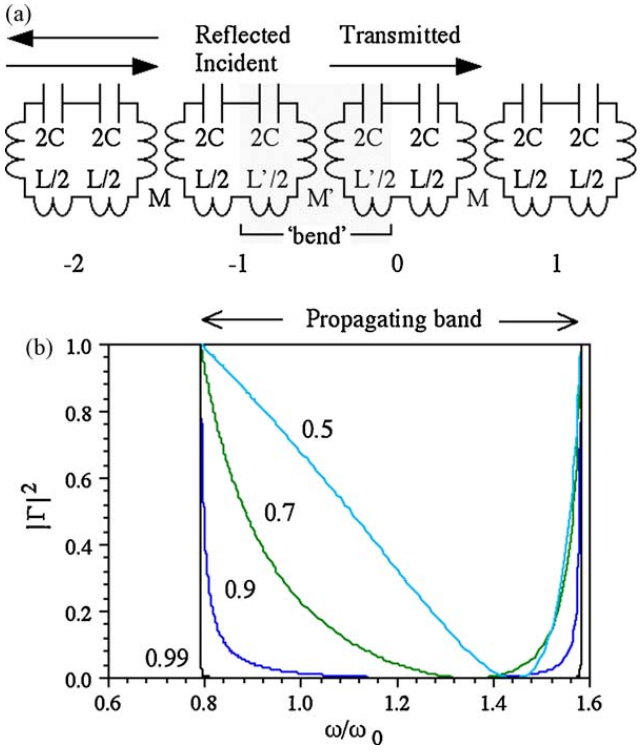

Fig. 5. (a) Equivalent circuit for a bend in a magneto-inductive cable; (b) frequency variation of the power reflection coefficient $|\Gamma|^2$ for different values of the inductance ratio $\mu=M'/M$.

In each of Figs. 4b and 5b, the plots for $\mu=0.99$ show low reflection across the band. In this case, it should be possible to construct high performance magneto-

inductive systems containing bends. However, we again note that a small discontinuity in μ requires precise placement of the elements in a discrete system, but is obtained automatically in thin-film cable merely provided the bending radius is not too small. On this basis, we may conclude that continuous cables are likely to have considerably better performance.

4. Experimental verification

In this section we verify the findings of the previous section experimentally using batch fabricated components. Due to the lack of stability of discrete-element waveguides, experiments were restricted to thin-film cables.

4.1. Thin-film components

Thin-film components including individual inductors and continuous magneto-inductive cables were fabricated by the UK company Clarydon (Willenhall, West Midlands), using double-sided patterning of copper-clad polyimide [10]. The starting material was 25 μm thick Kapton® HN (DuPont, Circleville, OH), coated on each side with a 35 μm thick pressure-bonded layer of copper. The copper was patterned by lithography and wet etching. Inductors were fabricated in panels containing 120 components, and cables were fabricated in 2 m lengths containing 24 parallel waveguides.

Each guide was equipped with input and output transducers, consisting of inductors $L/2$ made resonant at the element resonant frequency ω_0 using additional capacitors $2C$. Such transducers provide an excellent match between MI waveguides and resistive loads over the whole propagating band, allowing reflections from the input and output (which would otherwise lead to standing waves) to be largely suppressed and hence allowing additional small internal reflections to be distinguished. Electrical measurements were made with an electronic network analyser with 50 Ω characteristic impedance (Agilent E5061A).

4.2. Effect of bending on inductance

Changes in inductance were measured experimentally by making isolated inductors resonant using additional capacitors, and using an inductive probe to measure the change in resonant frequency following from a mechanical distortion. The inductor length, breadth and track-width were 60 mm, 5 mm and 0.25 mm, respectively, but a two-turn winding was used to increase Q-factor. The elements thus formed had a Q-factor of 62 at a resonant frequency of $f_0 = 70.5$ MHz. Inductors were wrapped around cylindrical plastic mandrels of differing radii, and the variations in their resonant frequencies were measured. The results are shown superimposed in Fig. 3b. A similar trend to the corresponding theoretical prediction is observed. L'/L is effectively constant until $r/h = 0.5$, and falls by around 9% over the range $0.5 > r/h > 0.1$. Resonant elements were also twisted, and little change in f_0 was seen. These results confirm that the properties of thin-film inductors are very stable, except of course to bending about an axis parallel to the conductors.

4.3. Effect of bending on cable

Experiments were then carried out on thin-film cables. Cable with an element length, element spacing and conductor spacing of 200 mm, 100 mm and 4.7 mm was used. Elsewhere [5], it has been shown that the resonant elements had a resonant frequency of $f_0 = 95$ MHz and a Q-factor of 48. The cable had a coupling coefficient $\kappa = 0.675$ and a mid-band impedance $Z_{0M} = 48.6\ \Omega$ and hence gave very low end-reflections when resonant transducers were used for coupling to 50 Ω impedance. However, some care was required to achieve repeatable results. Particularly, it was necessary to ensure that the SMA connectors used to connect to the measurement system did not distort the transducer elements. If this was done, very systematic behaviour was observed, and only the extreme cases need be discussed.

Initially, the network analyser was used as a signal source and a 50 Ω load was used as a termination. No systematic change in the reflection (S_{11}) could be seen when one or more 90° bends of different radii were inserted at different points in an otherwise straight cable, unless sections of the cable were brought close enough together for different elements to couple magnetically.

To see any change in performance, much more extensive bending was therefore investigated. Both the cable and the transducers were wrapped around cylindrical mandrels as shown in Fig. 5, using mandrel radii as small as 5 mm. In this last case, the bends are extremely tight, and it seems unlikely that any practical application would require smaller fractional radii. A spiral pitch of 10 mm (approximately twice the conductor spacing) was used, and the number of turns per period was $N = a/2\pi R = 3.18$ with $a = 100$ mm.

The network analyser was then used to measure both reflection (S_{11}) and transmission (S_{21}), using coaxial cable to construct any additional electrical links needed. Fig. 6 compares the frequency variation of the S-parameters for straight cable (thick lines) and a

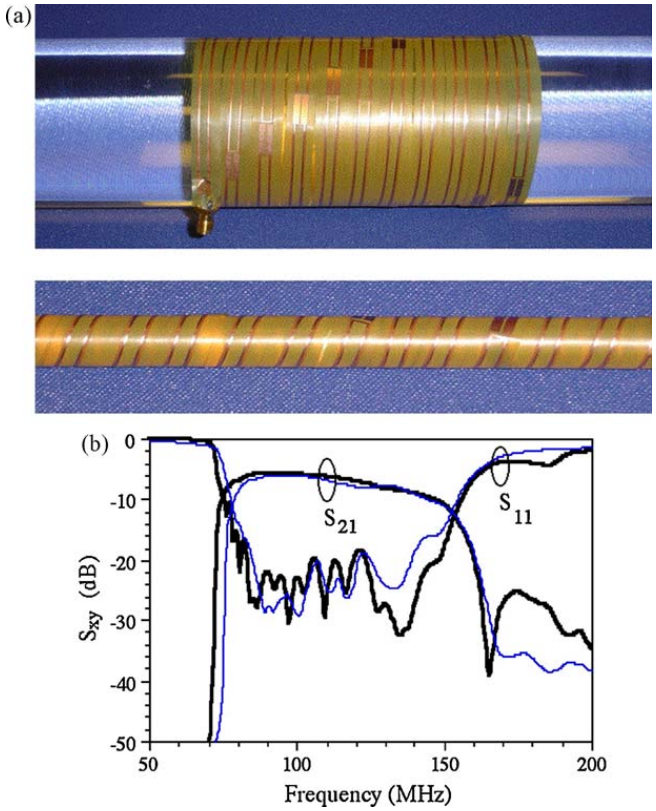

Fig. 6. (a) Experimental arrangement of two different spiral-wound bends in thin-film magneto-inductive cable; (b) frequency variation of *S*-parameters in 2 m lengths of straight cable (thick line) and spiral-wound cable (thin-line).

spiral-would cable with $R = 5$ mm (thin lines). Propagation takes place in a band ranging from ≈70 MHz to ≈160 MHz. In each case, the transmission is high, with a peak value of −6 dB, suggesting that propagation losses are low. For the straight cable, the reflection is below −20 dB, confirming the effectiveness of the transducers, and no standing waves are evident.

For spiral-wound cable, there is almost no change in either S_{21} or S_{11}, apart from a slight up-shift in frequency of the band due to the change in f_0 described earlier. There are no etalon effects, and it does not appear that adjacent turns of the spiral winding are coupled magnetically. There is however a slight reduction in the pass-band width, which suggests that the previous assertion concerning the stability of the ratio M/L may require further consideration. On this basis, it appears that thin-film MI waveguides with the right design are almost entirely insensitive to bending, a key requirement for practical application.

5. Conclusions

Bends in magneto-inductive waveguides have been shown present discontinuities in local parameters such as mutual or self-inductance that cause reflections. Equivalent circuits have been presented for abrupt bends in two forms of MI waveguide (based on discrete elements and continuous cable, respectively), and simple expressions have been presented for the reflection coefficient in each case. Discrete elements have been shown to offer relatively poor performance, due to the strong likelihood of differences in mutual inductance arising at bends, and the need to compensate for such differences using an overall reduction in the coupling coefficient. In contrast, thin-film magneto-inductive cable has been shown to be inherently stable, due to the limited effect of physical distortion on either the self-inductance or the mutual inductance, and low loss propagation through long lengths of spiral-wound cable has been demonstrated. These results suggest that thin-film cable is a promising format for exploitation of magneto-inductive waveguides.

References

[1] E. Shamonina, V.A. Kalinin, K.H. Ringhofer, L. Solymar, Magneto-inductive waveguide, Electron. Lett. 38 (2002) 371–373.
[2] M.C.K. Wiltshire, E. Shamonina, I.R. Young, L. Solymar, Dispersion characteristics of magneto-inductive waves: comparison between theory and experiment, Electron. Lett. 39 (2003) 215–217.
[3] R.R.A. Syms, I.R. Young, L. Solymar, Low loss magneto-inductive waveguides, J. Phys. D: Appl. Phys. 39 (2006) 3945–3951.
[4] M.J. Freire, R. Marques, F. Medina, M.A.G. Laso, F. Martin, Planar magneto-inductive wave transducers: theory and applications, Appl. Phys. Lett. 85 (2004) 4439–4441.
[5] D. Shelton, J. Tharp, G. Zummo, W. Folks, G. Boreman, Fabrication of periodic microstructures on flexible polyimide membranes, J. Vac. Sci. Technol. B 25 (2007) 1827–1831.
[6] M. Awad, M. Nagel, H. Kurz, Negative-index metamaterial with polymer-embedded wire-pair structures at terahertz frequencies, Opt. Lett. 33 (2008) 2683–2685.
[7] H. Tao, A.C. Strikwerda, C. Fan, C.M. Bingham, W.J. Padilla, X. Zhang, R.D. Averitt, Terahertz metamaterials on free-standing highly-flexible polyimide substrates, J. Phys. D: Appl. Phys. 41 (2008) 232004.
[8] X.G. Peralta, M.C. Wanke, C.L. Arrington, J.D. Williams, I. Brener, A. Strikwerda, R.D. Averitt, W.J. Padilla, E. Smirnova, A.J. Taylor, J.C. O'Hara, Large-area metamaterials on thin membranes for multilayer and curved applications at terahertz and higher frequencies, Appl. Phys. Lett. 94 (2009) 161113.
[9] F. Miyamaru, M.W. Takeda, K. Yaima, Characterization of terahertz metamaterials fabricated on flexible plastic films: towards fabrication of bulk metamaterials in terahertz region, Appl. Phys. Exp. 2 (2009) 042001.
[10] R.R.A. Syms, L. Solymar, I.R. Young, T. Floume, Thin-film magneto-inductive cables, J. Phys. D: Appl. Phys. 43 (2010) 055102.

[11] S. Weiss, P. Vernickel, T. Schaeffter, V. Schulz, B. Gleich, Transmission line for improved RF safety of interventional devices, Mag. Res. Med. 54 (2005) 182–189.
[12] R.R.A. Syms, L. Solymar, I.R. Young, Periodic analysis of MR-safe transmission lines, IEEE J. Sel. Top. Quant. Electron. 16 (2010) 433–440.
[13] I.S. Nefedov, S.A. Tretyakov, On potential applications of metamaterials for the design of broadband phase shifters, Microwave Opt. Technol. Lett. 145 (2005) 98–102.
[14] E. Shamonina, L. Solymar, Magneto-inductive waves supported by metamaterial elements: components for a one-dimensional waveguide, J. Phys. D: Appl. Phys. 37 (2004) 362–367.
[15] R.R.A. Syms, E. Shamonina, L. Solymar, Magneto-inductive waveguide devices, IEE Proc. Microwave Antennas Propag. 153 (2006) 111–121.
[16] M.C.K. Wiltshire, E. Shamonina, I.R. Young, L. Solymar, "Resonant Magnetic Concentrator" Progress in Electromagnetics Research Symposium, October 13–16, 2003, Honolulu, HA, USA, 2003, p. 469.
[17] M.J. Freire, R. Marques, Planar magnetoinductive lens for three-dimensional subwavelength imaging, Appl. Phys. Lett. 86 (2005) (art. 182505).
[18] R.R.A. Syms, T. Floume, I.R. Young, L. Solymar, M. Rea, Flexible magnetoinductive ring MRI detector: design for invariant nearest neighbour coupling, Metamaterials 4 (2010) 1–14.
[19] A.A. Oliner, Equivalent circuits for discontinuities in balanced strip transmission line, IEEE Trans. Microwave Theory Tech. MTT-3 (1955) 134–143.
[20] H.M. Altschuler, A.A. Oliner, Discontinuities in the center conductor of symmetric strip transmission line, IEEE Trans. Microwave Theory Tech. MTT-8 (1960) 328–339.
[21] P. Silvester, P. Benedek, Microstrip discontinuity capacitances for right angle bends, T junctions and crossings, IEEE Trans. Microwave Theory Tech. MTT-21 (1973) 341–346.
[22] A. Thomson, A. Gopinath, Calculation of microstrip discontinuity inductances, IEEE Trans. Microwave Theory Tech. MTT-23 (1975) 648–655.
[23] R. Horton, The electrical characterization of a right angled bend in microstrip line, IEEE Trans. Microwave Theory Tech. MTT-21 (1973) 427–429.
[24] H. Sasawa, H. Nakano, K. Koshiji, E. Shu, Transmission characteristics of CPW bends for various curvatures, IEICE Trans. Electron. E77-C (1994) 949–951.
[25] M.-D. Wu, S.-M. Deng, R.-B. Wu, P. Hsu, Full-wave characterization of the mode conversion in a coplanar waveguide right-angled bend, IEEE Trans. Microwave Theory Tech. 43 (1995) 2532–2538.
[26] K. Tomiyasu, The effect of a bend and other discontinuities on a two-wire transmission line, Proc. IEEE 38 (1950) 679–682.
[27] J. Lam, Equivalent lumped parameters for a bend in a two-wire transmission line: Part I. Inductance, in: AFWL Interaction Note 303, Air Force Weapons Laboratory, Kirtland Air Force Base, NM, 1976.
[28] J. Lam, Equivalent lumped parameters for a bend in a two-wire transmission line: Part II. Capacitance, in: AFWL Interaction Note 304, Air Force Weapons Laboratory, Kirtland Air Force Base, NM, 1977.
[29] T. Shiokawa, FDTD analysis of the transmission/radiation characteristics of 90° bent transmission lines, Electron. Commun. Jpn. 87 (2004) 11–22.
[30] R.J.P. Douville, D.S. James, Experimental study of symmetric microstrip bends and their compensation, IEEE Trans. Microwave Theory Tech. MTT-26 (1978) 175–182.
[31] A.A. Omar, Y.L. Chow, L. Roy, M.G. Stubbs, Effects of air-bridges and mitering on coplanar waveguide 90 degree bends: theory and experiment, in: Tech. Dig. 1993 IEEE MTT-S Int. Symp., vol. 2, Atlanta, GA, 1993, pp. 823–826.
[32] R.R.A. Syms, O. Sydoruk, E. Shamonina, L. Solymar, Higher order interactions in magneto-inductive waveguides, Metamaterials 1 (2007) 44–51.
[33] M. Kamon, M.J. Tsuk, J. White, FastHenry: a multipole-accelerated 3-D inductance extraction program, in: Proceedings of the 30th ACM/IEEE Design Automation Conference, Dallas, TX, 1993, pp. 678–683.